

EXPERIMENTAL PERFORMANCE EVALUATION OF A MODIFIED SOLAR ICE MAKER POWERED BY SOLAR ENERGY

Mohamed H. Ahmed, Ibrahim E. El-Seesy and Nagwa M. Khattab

Solar Energy Department, National Research Centre, Giza (Egypt)

1. Abstract

A prototype of a modified solar ice maker was constructed and tested for ice making purpose under Cairo climate. Activated Carbon and methanol have been used as the adsorbent - adsorbate pair. The system consists of adsorbent bed containing Activated Carbon (AC-35) mixed with very small particles of copper to increase the heat transfer through the adsorbent bed, copper condenser with circular fins, one valve and evaporator. A flat glass mirror reflector was used to increase the incident solar radiation on the adsorbent bed consequently the regeneration temperature, also an evaporative water cooler was used around the condenser to condense the adsorbate vapor within the desorption process in a hot day. Indoor and outdoor experimental tests were carried out on the solar ice machine. The experimental performance is presented in terms of gross solar coefficient of performance (COP) and quantity of ice produced. The test results show a daily ice production range from 1.38 to 3.25 kg ice/m² with a solar coefficient of performance (COP) between 0.07 to 0.11 under climate condition of daily solar radiation on the surface of the adsorbent bed range from 12.4 to 25.2 MJ/m² and daily average ambient temperature range from 21 to 35 °C. An increasing in the condensate methanol of about 1.1 liter was observed with increasing the regeneration temperature from 90 to 120 °C. Despite the simple technology used in the manufacture, the results show good and acceptable performance compared to the results of the research published.

2. Introduction

Cooling and refrigeration are an attractive and promise application of solar energy where the supply of solar radiation and the demand for cooling and refrigeration reach maximum levels in the same time. The solar ice maker to produce ice for food and fish conservations is one of the most suitable applications of solar energy in the coasts and remote area where there is no electricity grid. Different solar assisted cooling systems, liquid absorption or solid adsorption systems, were studied and tested with successes (Enibe, 1997, Meunier, 1998, Mesquita et al., 2006, Wang et al., 2000). However the use of liquid sorption for solar cooling induces two futures. First, liquid sorption cycles operate continuously, while solar energy is inherent transient during the day and vanish during the night, large heat storage must be installed between the solar collector and the generator. Second, the solution is most often circulated by a pump working all the day long, this pump consumes electricity that must be supplied by photovoltaic cells or reliable electricity network. Solid sorption work differently. First, the cycle is intermittent: heat is accumulated in the adsorbents resulting desorption of refrigerant vapor and only a cold storage is necessary for providing refrigeration over 24 hour period. Second, the cycle itself works without any mechanical input or moving parts. In addition to reliability, full autonomy with solar energy should be achievable, which is very attractive for installation in remote area.

The most important characteristic of adsorption systems, it is noiseless, not having any moving parts, not use any electricity, environment friendly and has the unique potential of utilizing low grade heat resources such as solar energy and waste heat. In comparison with mechanical vapor compression systems, adsorption systems have the benefit of saving energy, if powered by waste heat or solar energy, simpler control, no vibration and lower operation costs.

Nomenclature

A	Absorber area, (m ²)
AC	Activated Carbon
A–D	Points on Clapeyron diagram
C	Specific heat, (J kg ⁻¹ K ⁻¹)
L	Latent heat of evaporation of water, (J kg ⁻¹)
L.E.	Egyptian pound
G	Global solar radiation, (W m ⁻²)
m	Mass, (kg)
Q	Energy, (kJ)
T	Temperature, (C)
COP	Coefficient of performance
SCP	Specific cooling power, (W kg ⁻¹)

Subscripts

c	Condenser
e	Evaporator
g	Generator
l	water liquid

In comparison with liquid absorption systems, adsorption systems can be powered by a large range of heat source temperatures, starting at 50 and going up to 600 °C or even higher (Wang and Oliveira, 2006). Moreover, the latter system does not need a liquid pump or rectifier for the refrigerant, does not present corrosion problems due to the working pairs normally used, and it is less sensitive to shocks and to the installation position. These last two features make it suitable for applications in locomotives, busses, boats and spacecrafts.

Adsorptive refrigerating systems have been investigated by several research teams (Alghoul et al., 2009, Boubakri, 2006, Boubakri et al., 2000, Khattab, 2006) and applied in different fields (refrigeration, ice production, air conditioning, chillers...). In view of practical applications, the solid refrigeration system using activated carbon and methanol as working pair have the advantages of low desorption temperature and operation reliability. Although adsorption systems offer all the benefits listed above, they usually also have the drawbacks of low coefficient of performance (COP) and low specific cooling power (SCP). However, these inconveniences can be overcome by enhancing of the heat and mass transfer properties in the absorber, by increasing the adsorption properties of the working pairs and by better heat management during the adsorption cycle (Lu et al, 2006, Li and Wang, 2002). Thus, most research on this system is related to evaluation of adsorption and physical-chemical properties of the working pairs (Wang, 2005), development of predictive models of their behavior in different working conditions (Ej, 1996, Guillemot et al., 1987), and the study of the different kinds of cycles (Critoph, 1998, Wang et al., 1998).

Based on the results of above researches, one prototype was constructed and his performance was evaluated in laboratory and in real site. One reason of the drawback of the adsorption system is the low condensation of the methanol vapor during the adsorption process. For the above reason, this paper present an evaporative water condenser to condense the methanol vapor, very small copper particles were also mixed with the activated carbon to enhance the heat transfer through the carbon bulk. The sorbent bed was supplied with a glass mirror reflector to increase the incident solar radiation on the absorber surface and increase the regeneration temperature consequently. This paper presents an indoor and outdoor experimental results

obtained for a fabricated prototype of a solar ice maker for studying the performance at different operating and meteorological parameters

3. Principle of adsorption cooling system

The basis

The ideal adsorption cycle is usually represented in a $\ln P$ vs. $1/T$ diagram as shown in Fig. 1 where the isosters (the lines of constant methanol concentration x) are approximately straight lines. The cycle steps are:

- AB: isosteric heating of the adsorbent with increasing the pressure.
- BC: isobaric heating with decreasing the methanol concentration in the adsorbent bed.
- CD: isosteric cooling of the adsorbent with decreasing the pressure.
- DA: evaporating of the liquid at evaporating pressure and adsorbing the vapor through the adsorbent bed.

The heat is supplied during steps AB and BC, and the cold production occurs only in step DA. Thus, the simple cycle represented in Fig. 1 is intermittent. In solar powered machines, the cycle lasts for a whole day. The thick dashed diagonal line represents the saturation conditions of pure adsorbate. The other diagonal lines are the isosters.

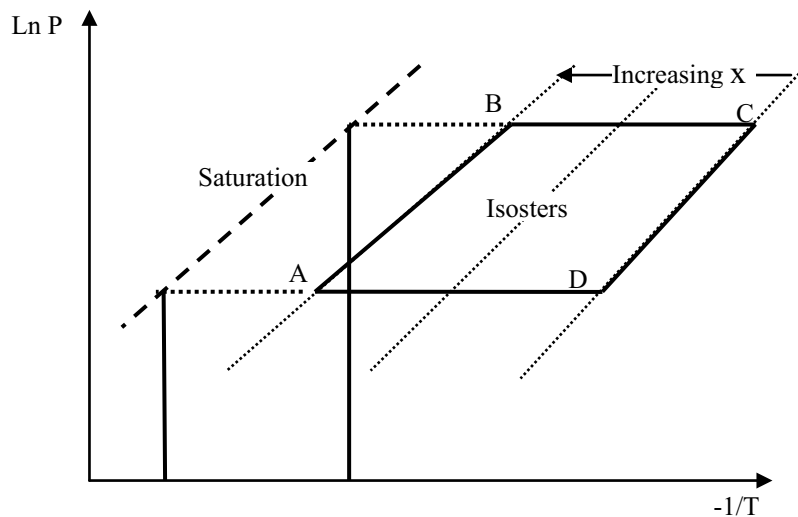


Fig. 1: The ideal adsorption cooling cycle in a ($-1/T$ vs $\ln P$) diagram.

4. Adsorbent–refrigerant pairs

The adsorbents and adsorbates (refrigerants) pair system is one of the most important elements of any solar ice maker or solar refrigeration systems. The main requirements of the refrigerant for those systems are: high latent heat per unit volume, low evaporating temperature and good thermal stability. The adsorbents must have high adsorptive capacity at ambient temperature and low pressures and a small capacity of adsorption at high temperatures and pressures. The suitable adsorbents are porous materials that should adsorb a range of refrigerants according to their molecular size and degree of polarization and exhibit some additional behaviors: wide concentration change within a small temperature range, reversibility of adsorption process for thousands of cycles, low cost, good thermal conductivity and so on. Appropriate working pairs are zeolite–water, zeolite–organic refrigerants, silica gel–water, salts–ammonia (ammoniated salts), activated carbon–methanol, metal–hydrogen (metal hydrides) and some other materials in solid sorption systems (Srivastava and Eames, 1998).

Choosing the adsorbent will depend on two basic factors:

- The temperature at which the evaporator must operate
- The regenerating temperature that the thermal source can possibly attain.

Among all these pairs of adsorbents and adsorbates, silica gel–water, activated carbon–ammonia (methanol), zeolite–water and calcium chloride–ammonia have been widely used in adsorption refrigeration systems utilizing solar energy and waste heat for the regeneration of the adsorbent bed. Zeolite–water and activated Carbon–methanol are the most used adsorbent–adsorbate pairs in refrigeration systems. These two pairs have entirely different physical and chemical properties: methanol is easily desorbed from activated carbon when it is heated, while in zeolite, the water is kept much longer.

5. Description of the solar ice maker

The solar ice maker consists of three main components which are solar collector containing the adsorbent bed, condenser and the evaporator.

The solar collector constructed from insulated wooden box (solar collector) with two transparent glass cover from the upper side. The solar collector containing the adsorbent bed is shown in Fig. 2. The adsorbent bed consists of twelve copper tubes with 600 mm length; the inner and outer diameters are 45 and 50 mm, respectively. The total absorbing area is 0.36 m². All tubes contain 4.8 kg of activated carbon mixed with very small copper particles in annular space. The outer surface of the copper tubes was black painted. An axial perforated copper tube was used and allocated at the axis of adsorbent tube to allow for the desorbed methanol vapor to flow out from the adsorbent bed toward the condenser. The inner diameter and length of the perforated copper tubes are 12 and 700 mm, respectively.

The condenser was fabricated from copper tubes with diameter and length of about 12 and 500 mm, respectively. Twenty five circular fins are used to enhance the cooling process for the condenser; the cooling can be achieved by either air or water. During the water cooling mode the condenser is immersed in clay container full of water as shown in Fig. 3.

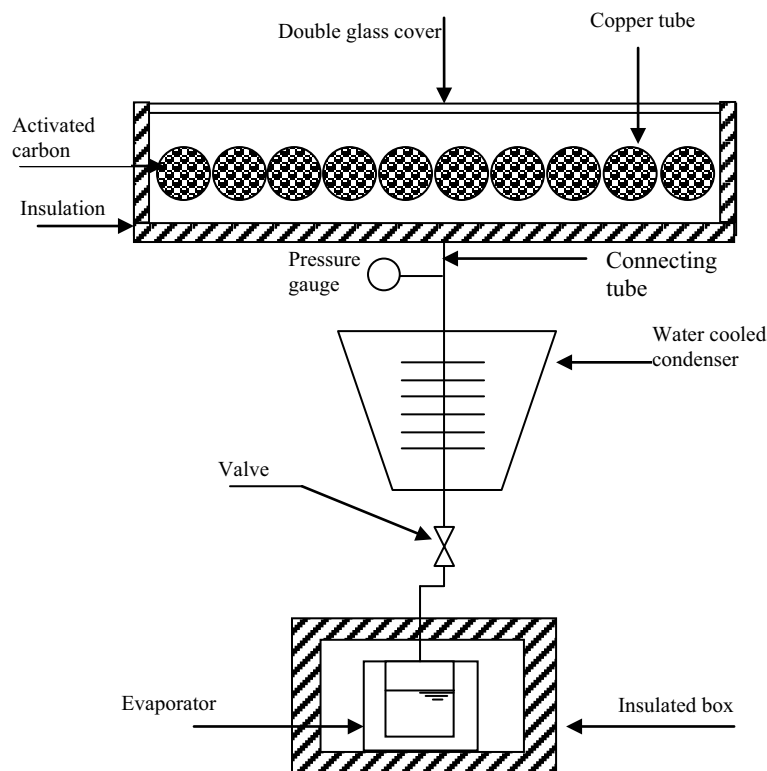


Fig. 2: Schematic diagram of the solar ice maker

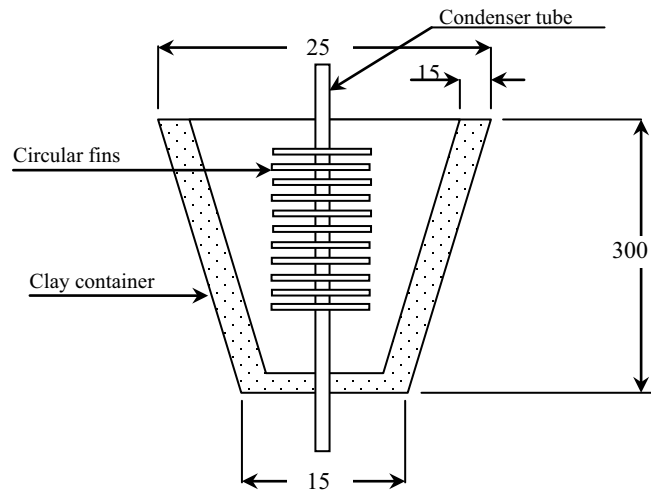


Fig. 3: A schematic view of the condenser.

The evaporator consists from two circular cylinders of copper various in diameter and length. The big circular cylinder has a diameter and length of 18 and 12 cm, respectively, while the smaller one has a diameter and length of 14 and 10 cm, respectively. The smaller cylinder put inside the big one forming a sump for accumulating the condensate methanol between the two cylinders, the water liquid to be frozen put inside the inner cylinder. The evaporator was placed inside an isolated box as shown in Fig. 2.

Two electric heaters of 1000 W were used to supply heat energy for indoor test only to simulate and control the regeneration temperature, an electric thermostat was used to adjust the regeneration temperature to the desired value. Flat mirror reflector was used to reflect the solar beam during the outdoor test for increasing the regeneration temperature. A manual valve was used between the evaporator and the condenser. Photographs for the solar ice maker and a sample of the ice produced are shown in Fig. 4



Fig. 4: Two photographs of the solar ice maker and ice produced

6. The performance of the solar ice maker

The performance of solar refrigerator is mainly decided by the total condensed refrigerant, the produced ice mass and the coefficient of performance (COP). The coefficient of performance of solar ice maker is expressed as the amount of cooling delivered (cold produced) divided by the amount of the heat input. The coefficient of cooling performance (COP) is calculated by the following formula

$COP = (\text{Cooling Delivered} / \text{Heat Input}).$

$$COP = \frac{Q_c}{Q_g} = \frac{m_l * [C * (T_c - T_e) + L]}{A \int G dt} \quad (1)$$

Where, Q_c denotes the heat removed from the cooled matter; and Q_g denotes the total solar radiation energy absorbed by the collector during one day operation, L denotes latent heat of fusion for water.

7. Experimental results

The experimental tests were carried out under both indoor and outdoor conditions. The indoor test was carried out using an electric heater as a heat source and thermostat to simulate and adjust the regeneration temperature, while the outdoor tests was carried out under the actual daily solar radiation and ambient temperature of Cairo.

7.1. Effect of the solar radiation

An actual daily solar radiation values various from 12.4 to 25.2 MJ/ m² day, at Cairo - Egypt (latitude 30° north), for different months through the year were selected for the study. The ambient temperature and solar radiation on the tilted surface of 30°, which represent the optimum annual tilt angel for Cairo, during two experimental test days for the test side are shown in Fig: 5 (one day in winter 21-Jan and other day in summer 21- Jun). From the figure we can observe that the difference between the available solar radiation failing on the tilted surface doesn't varies very much from Jan. to Jun. where the radiation increase in the winter by about 4.7 % at solar noon and decrease by about 16.9 % at evening and morning period. But due to the difference in the day length, the daily solar radiations on slop surface with angel of 30° varies from 15.7 to 23.4 MJ/m² from January to Jun, approximately. While in horizontal surface it varies from 12.4 to 25.2 MJ/m² from January to Jun, approximately.

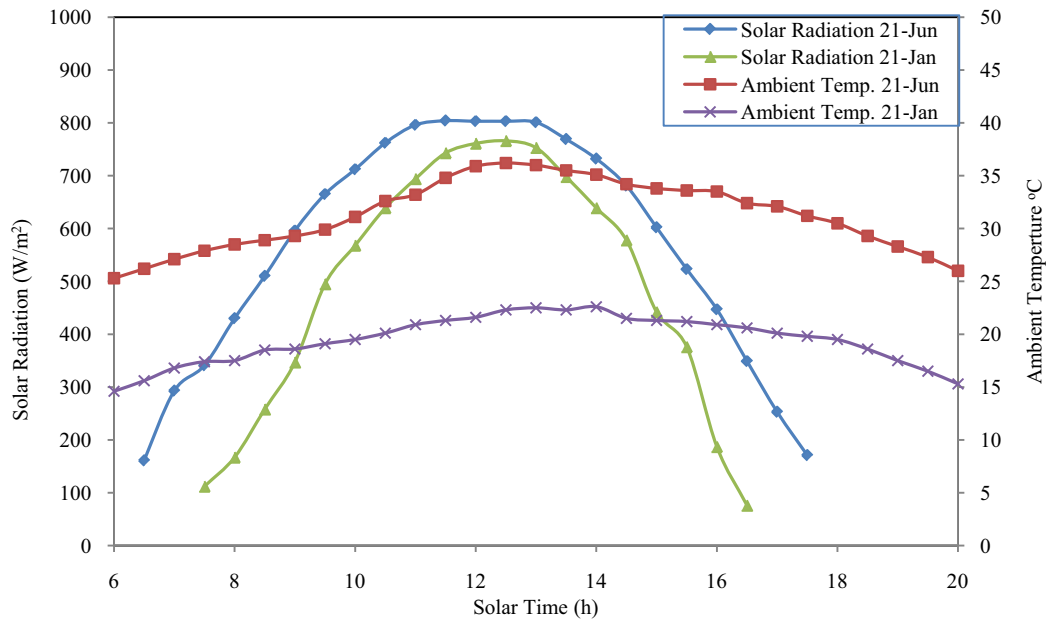


Fig. 5: Measured of solar radiation and ambient temperature versus solar time

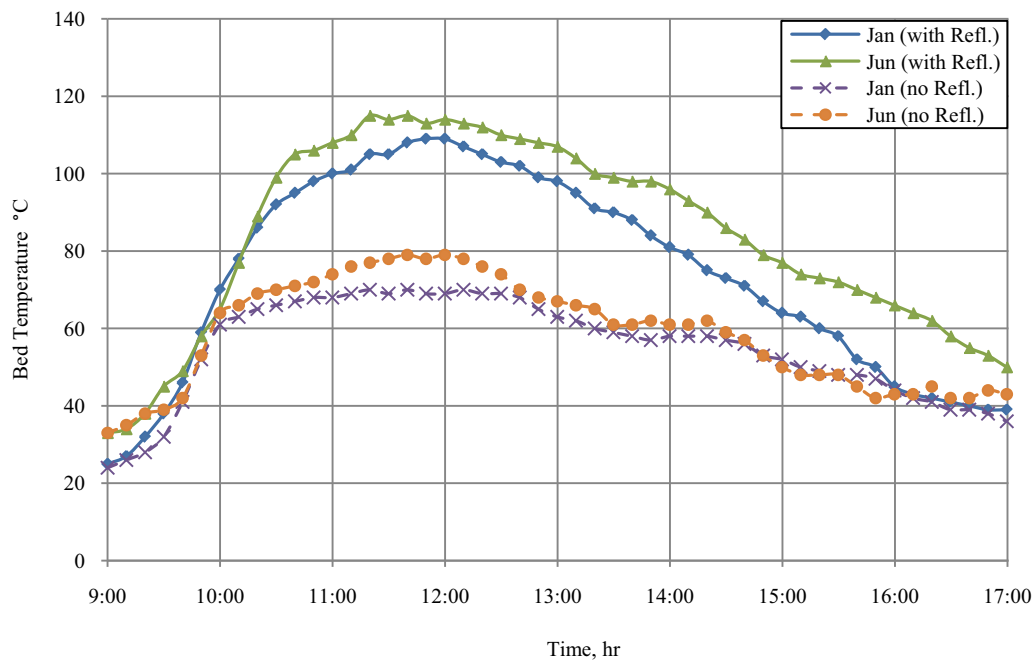


Fig. 6: Bed temperature during the desorption process for two days in the winter and summer

An increase in the bed regeneration temperature was achieved due to using a flat plate glass mirror reflector with a reflectivity of about 0.95 during the outdoor test. Fig. 6 illustrates the temperature profile for the adsorption bed with and without the flat mirror reflector for different two day in the summer and the winter. An increase in the bed temperature of about 38 and 41 °C was observed at solar noon during summer and winter, respectively.

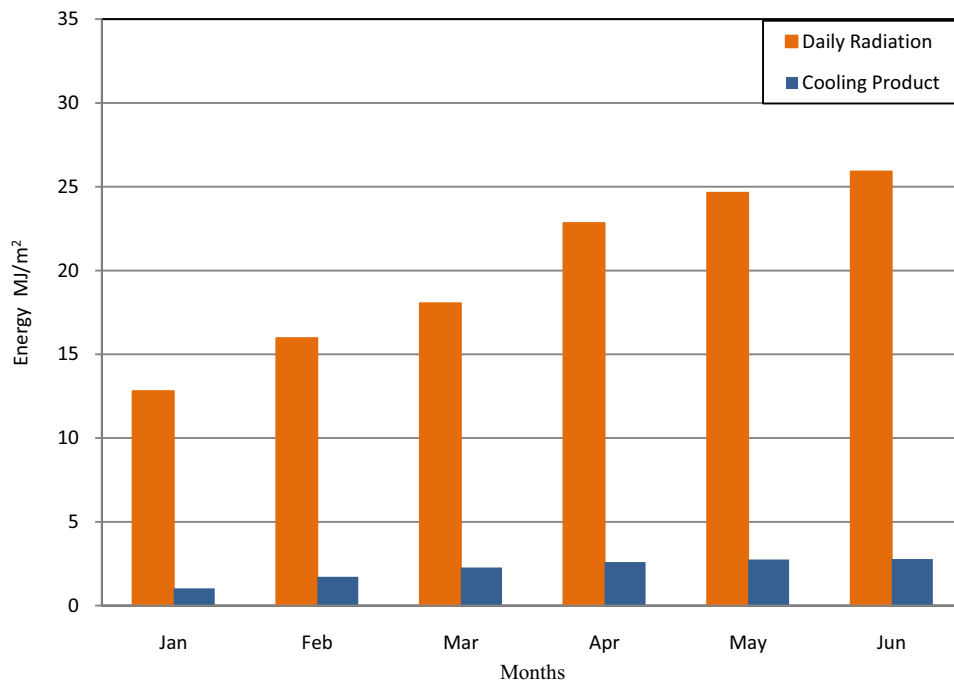


Fig. 7: Variation of daily solar radiation with the cooling product through different months

Effect of solar radiation on the performance of the ice maker has been studied experimental during the first six months of the year as shown in Fig. 7. The different months represent different daily solar radiation. The daily solar radiation varies from 12.4 to 25.2 MJ/m² from Jan to Jun, respectively. Consequently the cooling product per day varies from 1.03 to 2.77 MJ/m² as shown in Fig 7.

The variation of the daily solar radiation and its effect on the coefficient of performance for the ice maker and the daily ice produced are shown on Fig. 8. The COP increases from 0.07 to 0.11 with increasing the daily solar radiation from 12.4 to 19.1 MJ/m², respectively. The corresponding daily ice produced through these values of solar radiation range from 0.5 to 1.19 kg. This means the daily ice produced per unit area varies from 1.38 to 3.25 kg ice. Increasing the solar radiation from 19.1 to 25.2 MJ/m² leads to a decrease of the COP from 0.11 to 0.082, while the daily ice produced doesn't change.

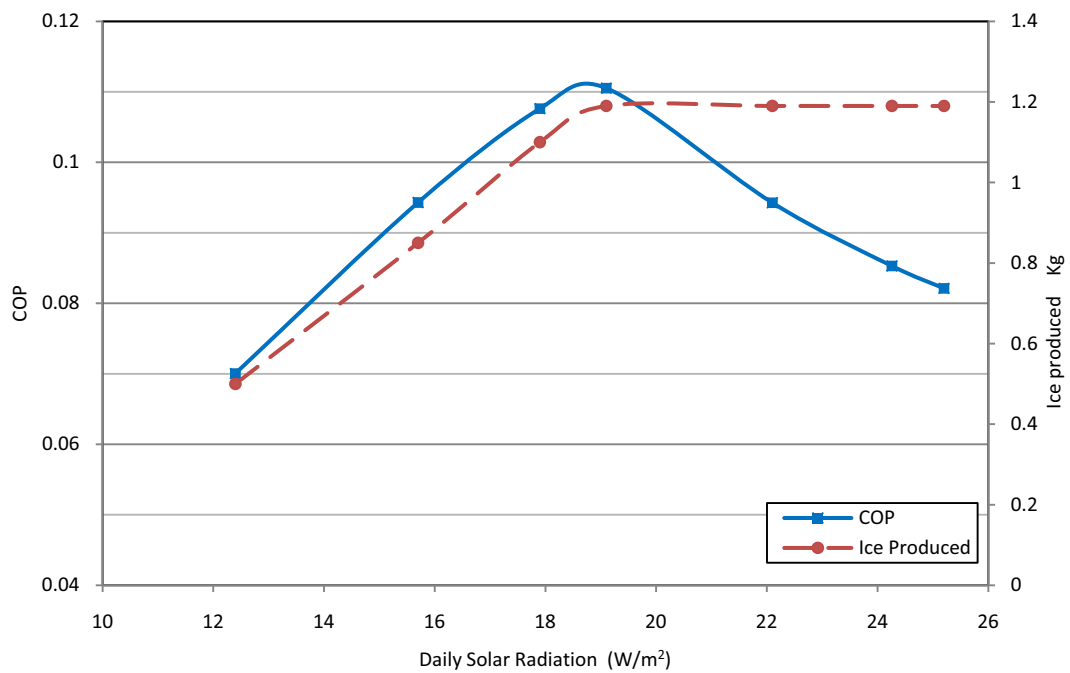


Fig. 8: Variation of COP and ice produced with daily solar radiation

7.2. Effect of the regeneration temperature

Indoor and outdoor tests were carried out for studying the effect of the regeneration temperature on the performance of the ice maker. As shown in Fig. 9, during the adsorption process, the water temperature in the evaporator was recorded through two adsorption processes for two different regeneration temperatures of about 100 and 120 °C. It can be observe that, the average water temperature decreasing through the evaporator with higher regeneration temperature of 120 °C is higher than that of the regeneration temperature of 100 °C by about 2.8 °C at the first two hours, then the enhancement in decreasing the water temperature became 4.1 °C at the next three hours. Then the evaporator temperature increases slightly due to higher heat loss through the wall of the evaporator box, and decreasing the absorption rate of methanol vapor, where the rate of heat loss become higher than the rate of evaporated methanol at this period. It can be also noticed that the evaporator temperature reach a minimum value of -5.3 and -7.5 °C for regeneration temperature of 100 and 120 °C, respectively.

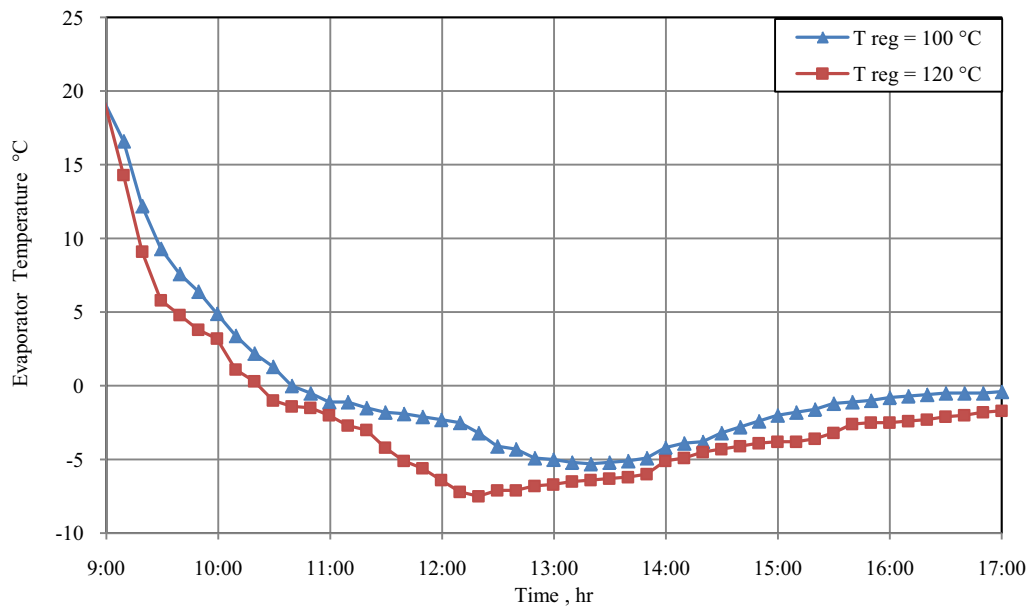


Fig. 9: Evaporator temperature during adsorption process

The alternation of adsorption and desorption process which carried out on the above described ice maker are presented in the Clausius –Clapeyron diagram as shown in Fig. 10. The short dashed straight line represent the methanol concentration in the activated carbon, the solid line cycle represent the desorption and adsorption process for maximum regeneration temperature of 100 °C while the long dashed cycle represent the desorption and adsorption processes for max temperature of 120 °C. It can be noticed that the maximum regeneration temperature effect the cooling effect, where for maximum regeneration temperature of 120 °C the cooling effect are greater than the cooling effect of 100 °C heating temperature case by about 518 kJ. The above observation effect also the quantity of ice produced where it increase with increasing the heating temperature. It can be also notice a rapid adsorption of methanol for the higher regeneration temperature case.

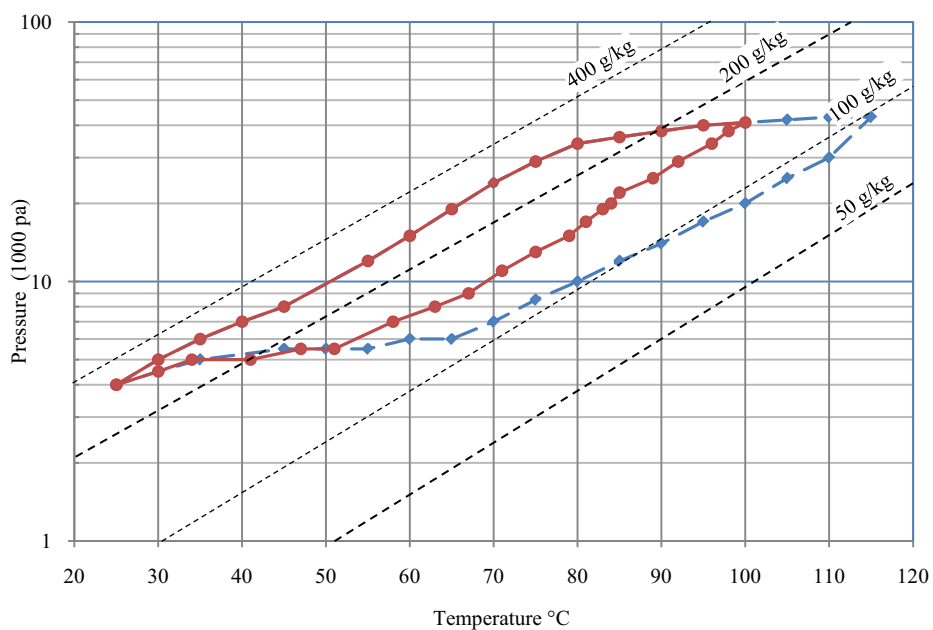


Fig. 10: Experimental desorption and adsorption cooling cycle for activate carbon–methanol

7.3. Effect of condenser cooling method and condensate temperature

Two methods were used for cooling the outer surface of the condenser. The first method is air cooling while the other is the direct water evaporative cooling method. Using direct evaporative water cooling to cool the condenser has a significant effect on the quantity of condensate methanol consequently the cooling power. A comparison between air cooling method and water cooling method was illustrated in Fig. 11 at ambient temperature of 25 °C. From the figure it can be observe that the increase in the methanol condensate due to using the evaporative water cooling method varies from 0.03 to 0.2 Liter for regeneration temperature varies from 90 to 120 °C, respectively. Increase the regeneration temperature above 120 °C results a decomposition of the methanol.

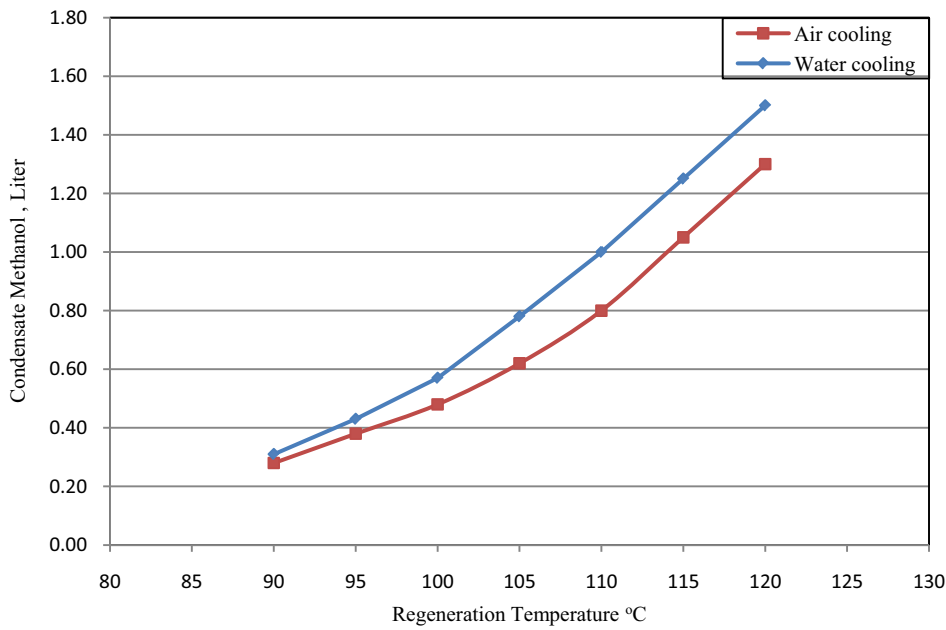


Fig. 11: Effect of cooling method on the condensate methanol at different regeneration temperature

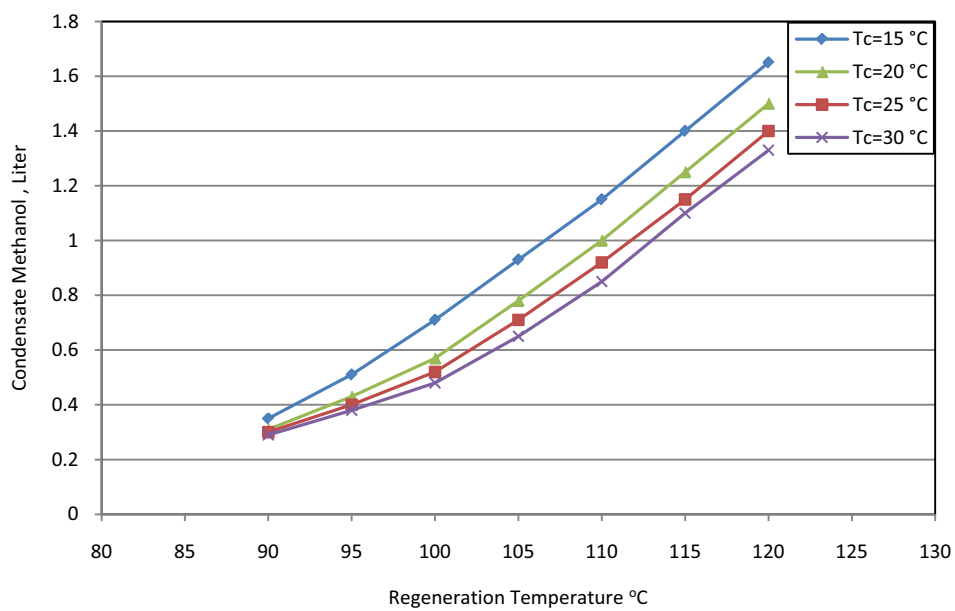


Fig. 12: Effect of condenser temperature on the condensate methanol for different regeneration temperature

The effect of condenser temperature on the condensate methanol was studied for different regeneration temperature as shown in Fig. 12. From the figure it can observe that decreasing the condenser temperature from 30 to 15 °C leads to increase the condensate methanol from 0.06 to 0.32 Liter for regeneration temperature range from 90 to 120 °C, consequently increases the cooling effect varies from 72 to 384 KJ. Increase the regeneration temperature above 120 °C results a decomposition of the methanol. The previous values vary for different condensing temperature as shown in Fig. 12. The effect of condensing temperature appears significantly at the higher regeneration temperature. For decreasing the condenser temperature from 30 to 15 °C, the percentage increase in the condensate methanol quantity varies from 20 to 24 % at regeneration temperature varies from 90 to 120 °C, respectively. An increasing in the condensate methanol of about 1.1 liter was observed with increasing the regeneration temperature from 90 to 120 °C

The cost of the solar ice maker is an important parameter for comparison with the conventional ice maker powered by electric. The comparison now will not be in favor of the solar ice maker in terms of cost and quantity of production to the size of the unit, but the solar ice maker is a fitting choice economically in places where there is no electricity grid.

Tab. 1: Cost of the main component of the solar ice maker

Item	Cost (LE)
Solar collector with steel supported frame	1150
Adsorbing bed from copper tube	1600
Activated carbon (3.6 kg)	250
Methanol (1.44 Liter)	200
Copper condenser	320
Copper evaporator	380
Wooden Isolated box	400
Total price	4250

Table 1 show the cost of the main component of the solar ice maker for 0.36 m² absorber area including the manufacturing cost. The total cost of whole ice maker is 4250 L.E around (720 \$). It can be notice that the main cost is from the solar collector and the adsorber bed.

8. Conclusion

The objective of this work has been to construct solar adsorption system for ice production in remote area of south Egypt like Nasser Lake where a high solar energy potential are available. A prototype of the solar ice maker was constructed to test the concept, identify problem carry out preliminary design optimization and measure performance under Cairo climate as an initial step before testing at the site of installation in southern Egypt.

The adsorption pair active carbon + methanol offer attractive possibilities for autonomous solar-powered cooling machines in Cairo climates. Addition of reflector mirror to concentrate solar radiation on the adsorber bed is necessary to increase the regeneration temperature from 75 to 110 °C at solar noon, but this increase is less gradually in the period before and after midday. Cooling the condenser using chilled water through direct evaporation reduces the temperature of the condenser by 4 °C, which leads to increase the methanol condensed consequently the cooling effect. This solar ice maker can produce about 1.38 to 3.25 kg of ice/m² each sunny day under the condition of about 12.4 to 19.1 MJ/m² daily solar radiation, which corresponding to COP of 0.07 to 0.11. For these reasons, this machine seems to be appropriate to be constructed for developing countries, despite the requirement of vacuum technology. The cost of manufacturing solar ice maker was estimated at around 4250 LE (US \$720) for a unit with 0.36 m² collector

area. The present experiments show a compatible results with that published in previous articles. In addition, this study shows that there is a great potential for using a solar energy for ice production

Acknowledgement

The supported fund provided for this work by the Arab Science and Technology Foundation (ASTF) is gratefully acknowledged. The authors gratefully acknowledge the staff of National Research Center (NRC) and the students of Helwan University who contributed to this work.

References

- Alghoul, M.A., Sulaiman, M.Y., Sopian, K., Azmi, B.Z., 2009. Performance of a dual-purpose solar continuous adsorption system. *Renewable Energy* 34, 920-927.
- Boubakri, A, Guilleminot, J.J., Meunier, F., 2000 Adsorptive solar powered ice maker: experiments and mode. *Solar Energy* 69, 249-63.
- Boubakri, A., 2006. Performance of an adsorptive solar ice maker operating with a single double function heat exchanger (evaporator/condenser). *Renewable Energy* 31, 1799-1812.
- Critoph, R.E., 1998. Forced convection adsorption cycles. *Appl. Therm. Eng.* 18, 799-807.
- EJ, H., 1996. Simulated results of a non-valve, daily-cycled, solar powered carbon/methanol refrigerator with a tubular solar collector. *Appl. Therm. Eng.* 16, 439-45.
- Enibe, S.O., 1997. Solar refrigeration for rural application. *Renewable energy* 12, 157-167.
- Guilleminot, J.J., Meunier, F., Paklesa, J., 1987. Heat and mass transfer in a non-isothermal fixed bed solid adsorbent reactor: a uniform pressure-non-uniform temperature case. *Int. J Heat Mass Transfer* 30, 1595-606.
- Khattab, N.M., 2006. A novel solar-powered adsorption refrigeration module. *App. Therm. Eng.* 80, 823-833.
- Li, M., Wang, R.Z., 2002. A study of the effects of collector and environment parameters on the performance of a solar powered solid adsorption refrigerator. *Renewable Energy* 27, 369-382.
- Lu, Z.S., Wang, R.Z., Wang, L.W., Chen, C.J., 2006. Performance analysis of an adsorption refrigerator using activated carbon in a compound adsorbent. *Carbon* 44, 747-752.
- Mesquita, L.C.S., Harrison, S.J., Thomey, D., 2006. Modeling of heat and mass transfer in parallel plate liquid-desiccant dehumidifiers. *Solar Energy* 80, 1475-1482.
- Meunier, F., 1998. Solid sorption heat powered cycles for cooling and heat pumping applications. *App. Therm. Eng.* 18, 715-729.
- Srivastava, N.C., Eames, I.W., 1998. A review of adsorbents and adsorbates in solid-vapor adsorption heat pump systems. *Appl. Therm. Eng.* 18,707-14.
- Wang, R.Z., LI, M., Xu, Y.X., Wu, J.Y., 2000. An Energy Efficient Hybrid System of Solar Powered Water Heater and Adsorption Ice Maker. *Solar Energy* 68, 189-195.
- Wang, R.Z., Oliveira, R.G., 2006. Adsorption refrigeration— An efficient way to make good use of waste heat and solar energy. *Progress in Energy and Combustion Science* 32, 424-458.
- Wang, R.Z., Xu, Y.X., Wu, J.Y., Wang, W., 1998. Experiments on heat regenerative adsorption refrigerator and heat pump. *Int. J Energy Res.* 22, 935-41.
- Wang, S.G., Wang, R.Z., Li, X.R., 2005. Research and development of consolidated adsorbent for adsorption systems. *Renewable Energy* 30, 1425-1441.